DEVELOPMENT OF IMPROVED SINGLE CRYSTAL GALLIUM PHOSPHIDE SOLAR CELLS

Quarterly Report No. 3

December 12, 1963 to April 12, 1964

Contract No. NAS3-2776

Placed by

NATIONAL AERONAUTICS AND SPACE ADMINISTRATION

Lewis Research Center

Cleveland, Ohio

MONSANTO RESEARCH CORPORATION

A SUBSIDIARY OF MONSANTO CHEMICAL COMPANY

DAYTON LABORATORY

DAYTON 7, OHIO

DEVELOPMENT OF IMPROVED SINGLE CRYSTAL GALLIUM PHOSPHIDE SOLAR CELLS

Quarterly Report No. 3
December 12, 1963 to April 12, 1964

Contract No. NAS3-2776

NATIONAL AERONAUTICS AND SPACE ADMINISTRATION
Technical Management
Space Power Systems Division
NASA - Lewis Research Center
Attention: Clifford K. Swartz

Report Prepared by: W. O. Groves and A. S. Epstein

Edited by: R. A. Ruehrwein

Work Performed by:
Central Research Department
MONSANTO COMPANY
St. Louis, Missouri

Requests for copies of this report should be referred to:

National Aeronautics and Space Administration
Office of Scientific and Technical Information
Washington, D. C. 20546
Attn: AFSS-A

NOTICE

This report was prepared as an account of Government-sponsored work. Neither the United States nor the National Aeronautics and Space Administration (NASA), nor any person acting on behalf of NASA:

A). Makes any warranty or representation expressed or implied with respect to the accuracy, completeness, or usefulness of the information contained in this report or that the use of any information apparatus, method, or process disclosed in this report may not infringe privately-owned rights; or

B). Assumes any liabilities with respect to the use of, or for damages resulting from the use of any information apparatus method or process disclosed in this report.

As used above, "person acting on behalf of NASA" includes any employee or contractor of NASA or employee of such contractor, to the extent that such employee or contractor of NASA, or employees of such contractor prepares, disseminates, or provides access to, any information pursuant to his employment or contract with NASA, or his employment with such contractor.

TABLE OF CONTENTS

LIST OF TABLES

LIST OF FIGURES

I. PURPOSE

This report presents the work done during the third quarter of the Single Crystal Gallium Phosphide Solar Cell program. The objective of this program is the development of an efficient solar cell operable at temperatures up to 500° C. The approach is to grow single crystal gallium phosphide by epitaxial deposition from the vapor phase on gallium arsenide substrate followed by removal of the gallium arsenide. Diffused junction cells are then fabricated and the photovoltaic properties of the cells are measured, ultimately up to 500° C. The design and performance of the cells are to be related to the electrical and optical properties of the gallium phosphide.

II. ABSTRACT

Single crystal gallium phosphide has been prepared by epitaxial deposition on single crystal gallium arsenide using hydrogen chloride in an open tube vapor transport process with phosphorus and gallium sources. Growth rate and electrical properties of the gallium phosphide are insensitive to phosphorus pressure during growth over a wide range but this may not be as true for the characteristics of solar cells fabricated from the material. An optimum vapor P/Ga mole ratio in the range of 0.6 to 1.4 is indicated by open circuit voltage measurements.

A very strong segregation of donor and/or acceptor impurities exists between growing surfaces of different orientations, the order for n-type carrier density being (111)B > (100) > (111)A. Differences in growth rate and thickness uniformity have also been found.

The vapor transport and epitaxial deposition of gallium phosphide by water vapor have been investigated briefly.

By correlating the GaP growth rate variables with solar cell electric and optical properties it has been possible to obtain solar cells having only the desired primary spectral response peak of 0.45 μ. These cells have produced the best electrical properties found thus far at room temperature in sunlight, namely, an open circuit voltage of 1.35 volts and a short circuit current density of 1.4 ma/cm^2.

The open circuit voltage-temperature relationships of the fabricated GaP solar cells have been examined. A temperature coefficient of open circuit voltage of about 3 millivolt/degree has been obtained which agrees surprisingly well with calculations made from a simple solar cell model assuming that only the energy gap of GaP is temperature dependent. While the slopes are in reasonably good agreement, the absolute value of the open circuit voltage obtained experimentally is much lower than that obtained using the simple model. With

improvement in the GaP material the difference between the theoretical and experimental values of V_{oc} has been narrowed to about 0.3 volts.

III. MATERIAL PREPARATION

The open tube, HCl transport process for growing GaP layers epitaxially on GaAs substrates and the technique for measuring their electrical properties have been described in Quarterly Report No. 1. Progress toward achieving a growth rate in excess of 0.50 μ/min. in order to obtain thick layers, factors affecting growth rate and surface perfection, and some results of doping experiments were described in Quarterly Report No. 2.

During this period major effort has been devoted to systematically investigating the effect on solar cell properties of phosphorus pressure during growth of the gallium phosphide crystals. While a growth rate of 0.60 μ/min. was demonstrated during growth of a 200 μ thick layer, emphasis has been shifted toward increasing deposition times as a means of obtaining thick layers. In addition, growth in <111> A and <111> B directions has been studied and transport of GaP by H_2O was investigated briefly.

A. Epitaxial Deposition

Run conditions and resulting growth rates for all HCl transport runs in the open tube system are summarized in Table I. Similar data for earlier runs are given in Table I, Quarterly Reports No. 1 and 2. The source, in all cases elemental Gallium (Alcoa, six 9's purity), was held at the temperature indicated. Phosphorus (American Agricultural Chemical Co., semiconductor grade red phosphorus) was evaporated into the gas stream at a lower temperature. Substrate temperatures and temperature gradients are based on thermocouples outside the tube in the deposition zone and a previous furnace calibration using a thermocouple inside the tube.

Flow rates of HCl and H_2 are based on flowmeter calibrations. Actual use rates of Ga average 84% of the indicated HCl flow rates. The phosphorus flow rate, derived from the weight losses of the phosphorus and gallium sources, is expressed as the P/Ga atom ratio in the gas stream beyond the Ga source but prior to any GaP deposition. In runs SC 31 through SC35, as discussed in Quarterly Report No. 1, the phosphorus flow rate decreased with time. The numbers given under P/Ga mole ratio are the values calculated for the start of the deposition, at completion, and the average during deposition. For runs SC36 through SC42, a new furnace system with a longer zone of uniform temperature allowed maintainance of a more nearly constant phosphorus evaporation rate; therefore, a single value for the P/Ga mole ratio is given. At the lower phosphorus pressures, the substrates were found to undergo extensive decomposition during the 1000° C pretreatment step, so for runs SC39 through SC41 the pretreatment was carried out under about 2cc/min of P_4 flow, the flow being continued for about 10 minutes of the deposition period. This would correspond to an initial P/Ga mole ratio of 4, not included in the value listed in the table.

The remaining columns list the time of deposition; layer thickness, an estimation based on cleaved sections of adjacent Hall bars and weight gain; growth rate in μ/min and in μ/cc HCl; and growth direction.

B. Discussion

The data for runs SC36 through SC42 indicate that growth rate (< 100 > direction) is insensitive to the P/Ga mole ratio(or phosphorus pressure) over the range of ratios between 0.79 and 3.12. Since in earlier runs P/Ga ratios varied within this same range it is not surprising that comparable growth rates have been obtained. At lower phosphorus pressures, as noted before in Quarterly Report No. 2, the

the growth rate does fall off. These runs were all of long duration, with two or more wafers included, so the growth rates do lie in the low end of the range previously found. The beneficial effect of supporting the wafers on a thick plate to bring them opposite the coolest region of the tube wall, as suggested by run SC30 in Quarterly Report No. 2, has not been realized.

The growth rate can be increased by increasing the temperature gradient (SC32 and SC33) and increasing the total flow rate (SC32). This attack for achieving thick layers has not been pursued, however, because of an indication of poorer solar cell properties, as will be discussed later, and the likelihood of increasing contamination at the higher source temperature required.

In run SC31 the effect of the reduced H_2/HCl ratio has been to sharply reduce the growth rate of GaP downstream, although that on the first wafer appears normal.

In run SC34 an attempt was made to lower the substrate temperature below that of the adjacent tube wall by using a heavy graphite support extending into the cooler zone downstream. The net effect, however, since it also extended into the hotter zone upstream, was to flatten out the temperature profile and slightly increase the substrate temperature. The growth rate was correspondingly reduced.

The effect of orientation on growth rate is indicated in Table I and given in more detail in Table II. Here the thickness of layers grown on pairs of adjacent Hall bars in the several runs is compared directly. The order of increasing growth rates is seen to be (111) B < (100) <(111)A although there is a wide variation in relative rates from run to run (greater than a factor of two) and between positions in the same run.

The uniformity of growth across full size wafers appears to be in the reverse order of the growth rate. This is particularly noticeable for the < 111 > A wafers. In a typical case (Figure 1) inside a thick

smooth outer rim, a region containing a high concentration of regular faceted holes is followed by a series of irregular steps as the thickness decreases toward the center. This non-uniform growth on the <111 > A surface may be related to rapid attainment of equilibrium with the gas stream causing depletion of that portion of the gas reaching the center of the wafer. If so, higher flow rates or a different flow pattern might improve the growth uniformity.

The surfaces of the <100 > wafers have been covered by the broad bumps previously described together with many smaller steeper bumps apparently nucleated during the deposition. The < 111 > B surfaces are covered by even broader, lower triangular pyramids and scattered polycrystalline nodules (Figure 2).

Several of the wafers of all orientations have broken spontaneously, apparently because of strain set up by the thermal expansion difference between GaP and GaAs. One < 111 > A wafer broke while the GaAs substrate was being etched off in nitric acid. It is evident that an annealing cycle must be introduced to obtain strain free GaP wafers.

C. Electrical Properties

Electrical properties of the epitaxial GaP layers prepared and submitted for solar cell fabrication are listed in Table III. All of these runs are undoped with the exception of SC33. The electrical properties of < 100 > layers, as determined by measurement of resistivity and Hall constant, are evidently independent of the phosphorus pressure within the range investigated, and average mobilities are equivalent to or higher than the best previously attained. In run SC33 an attempt was made to dope with Sn, the equivalent of 1.7×10^{19} atom/cc GaP being added to the Ga source. While little Sn, if any, was transported, the mobilities of the first two Hall bars are the highest yet measured, 230 and 130 respectively, indicating some gettering action. As discussed below,

there is not a direct correlation between mobility and solar cell characteristics, unfortunately, and high V_{oc} for a cell fabricated from SC33-3 was not realized. However, several cells having the best high temperature performance seen to date have been fabricated from this series, the best from SC40-3.

A segregation of impurities as indicated by a decrease in carrier level and in mobility with position (< 100 > orientation) was again noted. Data are summarized in Table IV.

A surprisingly pronounced difference in the electrical properties of GaP grown simultaneously on different orientations is shown by the data of Table III. The order of the segregation is the same as that which has been reported for GaAs[1] but the effect is an order of magnitude or more greater. The data are given in more detail in Table V where electrical properties of pairs of adjacent Hall bars are compared directly. The data also show the segregation of impurities in the < 111 > B growth. In two cases (SC37-5, -7 and SC42-5, -7) there is a pronounced decrease in carrier level with position accompanied by a doubling of the mobility. In one case (SC41-5, -7) an increase in carrier level is accompanied by a modest mobility increase. In most cases the < 111 > A deposits were of very high resistivity and, where measurements could be made, of very low mobility; data are insufficient to establish any trends.

D. H_2O Transport of GaP

Using the technique described by Frosch[2], GaP has been transported in wet hydrogen and deposited epitaxially on GaAs substrates. The source, GaP from Merck, was maintained at about 1085° C, < 111 > B and < 100 > oriented substrate wafers with adjacent Hall bars at 1066° and 1051° respectively, the temperature gradients being 5.5 and 6.2 ° C/cm. With a total hydrogen flow

rate of 380 cc/min and an initial water vapor pressure of 1.9×10^{-3} atm., the rate of source consumption, 2.8 mg/min., is in excellent agreement with the theoretical transport rate calculated from the equilibrium constant for the reaction given by Thurmond and Frosch[3].

The weight gain of the < 111 > B substrates is equivalent to a growth rate of 2.04×10^{-7} gm of GaP per cc of carrier gas and so of the same order as the rates reported by Frosch[2]. Heavy deposition on the cool wall depleted the gas stream sufficiently to cause extensive etching of the edges of the < 100 > wafer (Figure 4). The appearance of the < 111 > B deposits (Figure 3) with prominent development of < 110 > facets and large area of flat growth is equivalent to that reported by Frosch. The appearance of the < 100 > surfaces (Figure 4), however, is much superior, being free of the faceted pits.

Rather than inserting the wafers into the hot furnace according to the procedure of Frosch, the source and substrate were brought to temperature in a stream of hydrogen (380 cc/min) with phosphorus (2.3 cc P_4 /min) to prevent decomposition, the phosphorus flow being continued for 20 minutes after introduction of the water vapor. In this way a very smooth interface was formed (Figure 5).

The electrical properties of this material have not been obtained. The Hall bars, in the process of heat treatment for alloying In dots were converted to high resistivity. Probing the surface of the wafers with an ohm meter reveals the < 111 > B surface to be conducting, the < 110 > facets are nonconducting, while the < 100 > surface is conducting at the center with conductivity decreasing to zero at the etched sides.

E. Conclusions

Other conditions remaining constant, growth rate and electrical properties of deposited GaP layers are independent of phosphorus

pressures over a wide range.

Open circuit voltage of solar cells fabricated from the GaP is sensitive to some factor or factors, probably related to purity, not indicated by the mobility, and suggest an optimum P/Ga mole ratio in the range of 0.6 to 1.4 and a slow growth rate.

A very strong segregation of donor and/or acceptor impurities exists between surfaces growing in the <100> direction and the <111> B or <111> A directions. The best direction is still the <100> although with significant improvement in purity the <111> B might be preferred.

A significant improvement in structure and in economy of source material might be achieved by using an H_2O transport system rather than HCl transport but this is offset by the difficulty of working at the higher temperature required and the problem of maintaining purity at this high temperature.

IV. SOLAR CELL FABRICATION

The procedures for fabricating GaP solar cells as given in the first and second quarterly reports have been followed in this period.

A list of cells fabricated in this period and the conditions under which they were diffused are given in Table VI.

Experiments using gallium-zinc alloys as a source to optimize on the zinc surface concentration have produced no advantages over the zinc-phosphorus alloys at this stage and the latter has been continued as the zinc source for making p-n junctions. Zinc surface concentrations of the order of $10^{18}/cm^3$ have produced the best cells found thus far.

Base material having a carrier concentration in the low 10^{16} range with a mobility of about 100 has thus far produced the best cells.

V. SOLAR CELL MEASUREMENTS

In Quarterly Report No. 2 it was shown that the GaP solar cells fabricated during the course of this program fall into two categories,

those having the principal spectral response at about 0.45 microns and those having the principal response at about 0.7 microns. For convenience, these two types of cells can be referred to as 0.5 μ response cells and 0.7 μ response cells. The 0.5 μ response cells generally have exhibited a much smaller photocurrent density (J_{sc} of about 0.1 ma/cm^2) as compared with the 0.7 μ response cells (up to 5 ma/cm^2) using a tungsten lamp source. From the spectral response data for the two types of cells (summarized in Quarterly Report No. 2) it was to be expected that the photocurrent from the 0.5 μ response cells would be relatively weak with a tungsten light source which has a peak intensity (through water) at a wavelength of about 0.8 micron. Accordingly, measurements have now been made in sunlight which has a peak intensity at a wavelength of about 0.45 micron. Total intensity of the sunlight was measured with a standard silicon solar cell and generally was between 80 and 100 mw/cm^2. Results are summarized in Table VII for a number of 0.5 μ response cells and for one 0.7 μ response cell, NA 21 SC21-3. As expected the photocurrent in sunlight is much greater for the 0.5 μ response cells as compared with tungsten illumination. The response of the 0.7 μ response cell is relatively independent of the source. The measured open circuit voltage of both types of cells does not change appreciably with the type of source used.

VI. OPTIMIZATION OF GaP GROWTH CONDITIONS WITH SOLAR CELL ELECTRICAL CHARACTERISTICS

Using the sun as a source and with a series of Schott color filter glasses to delineate the wavelength response of the GaP solar cells, it was found that, with the exception of a few solar cells having their main response at 0.7 μ, most of the cells contribute mainly to the short circuit current from response to wavelengths less than 0.5 μ. This is what one expects from theory. However, of additional interest is

the observation that the response peaks of 0.53 μ, 0.58 μ and 0.7 μ (broad), in these cases account for less than 5% of the current and in some cases less than 1%. However, while they may not contribute in these cases to the current directly they can in a detrimental way influence (reduce) the current and/or voltage.

Since these response peaks have in some cases been influenced by altering the zinc concentration it is felt that the spectral response peaks of 0.55 μ, 0.58 μ and 0.7 μ (broad) found in the solar cells are likely associated with impurities or imperfections in the lattice. For ideal solar cell action the response only to the main band edge is desired and hence the removal of the response in the longer wavelength region by varying the crystal growing conditions and also their specific influence on the solar cell are the subject of this section.

The effect of some of the growth conditions used in making epitaxial GaP (i.e., the gallium and phosphorus source temperature and the hydrogen flow rate) on the solar cell spectral response (peaks) and the short circuit current density (J_{sc}) are shown in Table VIII. For these series of experiments the regular diffusion cycle and our standard fabrication technique have been used in making the solar cells ** .

One notes from Table VIII that for our particular growing technique a (Ga) source temperature of about 900° as compared with the higher source temperature of 935° or 975° appears to give the best combination of major response peak (0.45 μ) and highest short circuit current in sunlight. A hydrogen flow rate between 95 cc/min and 500 cc/min appears, on the basis of Table VIII, to provide the most desirable solar cell properties. It is beneficial

---

** See second quarterly report.

to see whether one cannot narrow the optimum hydrogen flow rate by considering additional electrical parameters such as the effect of J_{sc} with temperature and the solar cell conversion efficiency* (in sunlight) at room temperature. In Table IX are listed those samples grown at a (Ga) source temperature of approximately 890° and having only the characteristic 0.45 μ peak response. The above electrical properties are compared for the various hydrogen flow rates from 95 cc/min to 500 cc/min. Since ideally we would expect the short circuit current to change only little with temperature in the range to 300° C, our criterion should be based on looking for samples with small slopes of J_{sc} vs. 1/T. In Table IX we have indicated the slopes from the J_{sc} vs. 1/T curve assuming that $J_{sc} \alpha e^{-\Delta E/kT}$. It will be seen that the samples having short circuit currents greater than 0.5 ma/cm^2 also exhibit the shallowest slopes and only a single slope ($\sim$0.05ev), whereas those generally with short circuit current densities less than 0.5 ma/cm^2 have either two slopes or a higher slope of .08 ev. It is noted that the samples with the highest or the multiple slopes have been grown with the highest hydrogen flow rate (500 cc/min). There is one exception and that is sample NA30 SC31-3 which in spite of the apparent higher J_{sc} has exhibited no simple dependence of J_{sc} with temperature. The curve was found to be irregular, staying constant then rising, then remaining constant. A check of the conversion efficiency showed in spite of the high J_{sc} and V_{oc} (see following discussion and Table XI) a value of only 0.45% which is about half of that expected. The sample unexpectedly revealed an apparent high internal series resistance of unknown origin. Since another sample grown under

---

* Measurement made from open window between 11:00 a.m. and 3:00 p.m. with sample pointed toward sun. A 10% standard silicon solar cell was also measured at the same time to determine the solar intensity - if the incident intensity was lower than 80 mw/cm^2 measurements were not taken.

similar conditions gave poor results it appears that the flow rate of hydrogen of 95 cc/min is not a reliable rate to use. From the data summarized in Table IX, material grown with hydrogen flow rates between 150 cc/min and about 300 cc/min seem to give the highest values of efficiency. For our work a hydrogen flow rate of about 300 cc/min has been adopted as standard.

Another growth variable that was considered is the phosphorus flow rate (or the P/Ga mole ratio). Data are being obtained to optimize this variable with the other growth conditions kept constant - that is, the Ga source temperature has been maintained at about 900° C, hydrogen flow rate at 300 cc/min and HCl flow rate fixed at about 2 cc/min. A < 100 > crystal orientation is being used. The results as presently available are shown in Table X with V_{oc}, J_{sc} and spectral response compared. It can be seen that with a phosphorus flow rate broadly between 0.3 and 0.6 cc/min (or expressed as a P/Ga mole ratio between 0.6 and 1.4) the best electrical properties and spectral response are obtained.

Thus far the effect of the longer wavelength spectral response (0.53, 0.58, 0.7) on the magnitude of the short circuit current has not been tacitly brought out, nor has it actually been determined explicitly how the presence of these responses are detrimental to solar cell performance. From Table VIII it would appear that in certain cases even with the presence of these responses, short circuit current densities of 0.5 to 1 ma/cm^2 are observed in the sun. On the other hand we note that in some of the cases there appears to be a connection between the presence of response peaks at 0.53 μ, 0.58 μ and 0.7 μ and the low magnitude of the current obtained. These are associated generally with the samples which either have anomalously high mobilities, are initially p-type or have very high resistivity epitaxial layers.

To more clearly show the possible effect of these extraneous responses on the GaP solar cell we consider the relationship of the measured open circuit voltage and the value of the voltage at the knee (V_{knee}) of the forward I-V trace of these samples (i.e., where there is a change in slope and the current increases more rapidly than the voltage. All of our data was taken with a Tektronix Scope Model No. 536 with the current scale at 0.2 ma/cm and the voltage at 0.5 volts/cm. It is known that this value should closely approximate the built in voltage of about 1.5 v for GaP for an ideal case. Further, the open circuit voltage measured in sunlight should be in reasonable agreement with V_{knee} if the internal cell resistance is low.

In Table XI are listed the parameters V_{knee}, spectral response peaks, V_{oc} (sunlight) and J_{sc}(sunlight) for some of the above samples. Several effects are noted: (1) In those samples where only the major spectral response is found one observes good correlation between V_{oc} and V_{knee}. (2) The presence of the extraneous peaks appears to be associated with disagreement between V_{knee} and V_{oc}. This may suggest that if we associate these response peaks with impurities, it is possible the location of these impurities (i.e., whether in the p, space charge or n region) and its position with respect to the Fermi level in these regions may determine its role. It is also possible that photoconducting effects in addition to a photovoltaic effect may occur. (3) In general the presence of these response peaks appears to lower the open circuit voltage below that observed when only the 0.45 response is present. It therefore appears that the open circuit voltage should be a sensitive indicator of sample purity and that these extraneous responses are generally undesirable.

VII. SOLAR CELL EVALUATION

A list of cells evaluated in this period are given in Table XII. The V_{oc}, J_{sc} under both tungsten light and sunlight are reported together with the spectral response peaks and the cell area. In some of the cases the conversion efficiency measured in the sunlight at a temperature of 23° C is reported. The solar intensity used in determining the efficiency was obtained with a standard 10% silicon solar cell and only when intensity levels were 90 mw/cm^2 or greater were measurements recorded.

The highest value of short circuit current density achieved at 23° C for cells with 0.45 μ response is 1.4 ma/cm^2. The best room temperature open circuit voltage obtained on GaP cells has been 1.35 volts. A room temperature efficiency of 1.1% is the highest thus far obtained. These values have been obtained for cell NA31 SC34-3. The cell area of this sample is 0.57 cm^2 which is larger than those tested previously.

In Table XIII are shown the characteristics of four cells delivered to Lewis Research Center during this period - three of the cells have the desired 0.45 μ response, while the fourth cell is characterized by the 0.7 μ response.

It will be noted that Sample NA 32 SC 34-5, grown at the same conditions as NA 31 SC 34-3, has about half the short circuit current density. A possible explanation for this difference may lie in two other observations: (1) the p-layer concentration is almost a factor of three greater in sample NA 32 SC34-5 than in sample NA 31 SC34-3, (2) the junction depth is greater in NA 32 SC34-5 than in NA 31 SC34-3. On the basis of the above two observations the difference in short circuit current density in the two samples could arise either because of carrier absorption or because of the difference in junction depth between the two samples.

A. Temperature Coefficient of Open Circuit Voltage

A meeting was held with personnel of the Lewis Research Center during this period to review the status of the program. Since it is now possible to make solar cells exhibiting response only at the fundamental absorption and with reasonably large open circuit voltage it was agreed that principal effort should be devoted to establishing the influence of temperature (up to 500° C) on the open circuit voltage. The feasibility of utilizing gallium phosphide solar cells at high temperatures can then be determined from this information.

From solar cell theory and for an ideal junction the open circuit voltage V_{oc}, is given by the following expression:

$$V_{oc} = \frac{kT}{q} \ln \frac{J_L n_n}{2.23 \times 10^{31} qT^3 \left(\frac{D_p}{\tau}\right)^{1/2} e^{\frac{-Eg-(\frac{dEg}{dT})\Delta T}{kT}}} \qquad (1)$$

where T is the absolute temperature, n_n is the carrier concentration of the base material, D_p is the hole diffusion constant, $\tau = \tau_p = \tau_n$ is the minority carrier lifetime, Eg is the energy gap, $\frac{dEg}{dT}$ is the temperature coefficient of the energy gap and J_L is the short circuit current density.

Equation 1 has been calculated for gallium phosphide assuming an energy gap of 2.25 ev at 300° K, a temperature coefficient of energy gap of -5.4×10^{-4} ev/deg[5] and with τ_p taken as 10^{-10} sec. The results of the calculation are given on the linear plot of Figure 6. At 300° K an open circuit voltage of 1.68 volts would be expected for gallium phosphide.

It should be mentioned that in spite of the fact the major absorption occurs at the higher energies ($\lambda \approx 0.45\ \mu$) and more nearly

corresponds to the "direct transition" band gap (contrary to some of the other semiconductors), the lower band energy of 2.25 ev was used in the calculation since it is assumed that electrons with higher energies will lose the energy difference between 2.75 and 2.25 ev through some energy consuming phonon interaction process in changing from upper to lower conduction band.

One can express the voltage-temperature plot of Figure 6 in terms of the simple linear relation:

$$V_{oc} = V_{oc(23)} - \beta(t-23) \qquad (2)$$

where V_{oc} is the open circuit voltage at any temperature t, $V_{oc(23)}$ is the open circuit voltage at 23° C, t is the temperature in degrees centigrade and β is the temperature coefficient of the voltage.

On the basis of Equations 1 and 2 and Figure 6 we would expect for a gallium phosphide solar cell a β of about 3.0 mv/deg. In the succeeding paragraphs we shall discuss our experimental results obtained with cells having the 0.45 μ response.

The cells for temperature measurements are nominally mounted in a special cell holder which can be inserted into a cylindrical muffle furnace (Hoskins). Provisions have been made for a chromel alumel thermocouple inserted under the solar cell to record cell temperature. The top of the cell holder has an opening so that a source suitably mounted and focused at the top of the furnace can provide the desired intensity through a glass filter to the cell. For the source a G.E. Projector Spotlight, 150 PAR/SP, has been used. The variation of intensity can be accomodated by adjusting the separation between the source and sample. An experiment was carried out at two temperatures (23° C and 225°C) to check the relationship

and determine where the V_{oc} of the cell saturates with distance, L. Figure 7 is a plot of these measurements. A check was also made at the higher temperature (225° C) in order to determine whether with the expected shift of the peak response to longer wavelength at higher temperature the source setting at 23° C would still be valid at higher temperatures. Experiment showed that it was. In fact, as expected, saturation of V_{oc} with distance occurred at a greater distance (lower intensity). It will be noted that even with the largest separation (L = 20") (lowest intensity utilized) there is less than a 10% variation in V_{oc}. The setting normally used was L = 10" or within the saturation region. To avoid any undue heating the light was turned on only to take a reading and then for only a short time (a few seconds).

In order to further check ourselves, open circuit voltage measurements with temperature were made using the sun as a source. The measurements were taken starting at 12:30 p. m. with the sample directly illuminated by the sun. The sun was south to southwest and the day was bright and clear. From monitoring with a standard silicon solar cell, the intensity was found to be 90 mw/cm^2. The results of the measurements and the comparison with the tungsten source illumination with the source-sample separation set at L = 10" and L = 20" are shown in Figure 8 for sample NA33 SC 37-3. Good agreement was found between sunlight measurements and the L = 10" measurements. It was also noted that there is at most only a few percent difference in V_{oc} between the L = 10", sunlight measurement and the L = 20" measurements.

At lower temperature (< 150° C) some differences were noted in the measurements between sunlight and the L = 10" case. This may be due to surface effects. Such large differences have not always been

observed although some bending is generally noted around room temperature.

In Table XIV are listed the experimental data on β, the temperature coefficient of open circuit voltage for those cells having the 0.45 μ response. Also given are the open circuit voltage at 23° C, the maximum temperature to which the cell was taken and the V_{oc} at that temperature. In the last column the initial n-type carrier concentration of the base material is reported.

One notes that β appears to vary from around 2.5 mv/deg to a maximum of 4.4 mv/deg. The majority of the cells appear to be close to the value of 3 mv/deg. In fact taking into account the uncertainty in the slopes, aside from sample NA30 SC31-3, most samples fall well within the calculated value of β.

It is also to be noted from Table XIV that generally with a lowering of the starting carrier concentration which as noted in an earlier section is a sign of improved purity, the maximum temperature at which an open circuit voltage of about 0.30 is recorded, has been gradually raised.

It is of interest to examine the V_{oc}-temperature results obtained experimentally with that expected from theory as denoted by Eq. 1. This comparison is shown in Figure 6. The experimental and theoretical curves give about the same slope (β = 3 mv/deg) as already noted and this would tend to imply that the largest effect on temperature is the change in energy gap - this being the only factor in the expression in Eq. 1 permitted to vary with temperature (in first approximation). A second factor needs to be examined in Figure 6 and that is the absolute difference in magnitude existing (at any temperature) between that expected theoretically and

that obtained experimentally. There is, for example, a difference of about .3 volts between the best experimental observation and theory. The difference cannot be simply accounted for in terms of lifetime or diffusion length as permitted in Eq. 1. While it is possible to account for the difference in terms of another phenomena such as recombination currents as has been pointed out by Wysocki and Rappaport[6] it is also of advantage to examine the spread in voltage of GaP solar cells shown on the figure. One may generally note from the data (Table XIV for example) that with increasing purity, improved structure and better control of crystal growing conditions the V_{oc} - temperature curves have generally improved and higher open circuit voltages have been obtained. Thus hopefully, with better growing and fabrication procedures V_{oc} might be expected to more nearly approach the theoretical curve of Figure 6.

One can perhaps more clearly see the picture in perspective by reference to Figure 9 where calculated and experimental curves of V_{oc} vs. temperature for GaAs and silicon solar cells are presented. The calculated curves for GaAs and silicon are based on the work of Wysocki and Rappaport[6] and utilize Equation 1. The lifetime of GaAs is taken as 10^{-8} sec and that of silicon as 10^{-7} seconds. The silicon solar cell experimental data is also taken from reference (2). The GaAs solar cell experimental data is taken from Gobat, et al[7].

From Figure 9 there is reasonable agreement between the theoretical curve and experimental data on GaAs and silicon solar cells whereas in the case of GaP, there is a wide difference as already pointed out. It is, however, of interest to note that far greater control of crystal growth, structure and purity has been obtained with silicon and GaAs than with GaP. It would then appear that with improved material the GaP solar cell might ultimately be expected to approach the theoretical curve expected for the GaP solar cell V_{oc}-temperature relationship.

VIII. APPARATUS

An Eppley NIP Pyrheliometer has been ordered during this quarter to permit more quantitative sunlight measurement to be made.

IX. FUTURE PLANS

The major problem remaining is improvement of purity. The following steps are planned:

(1). To try Monsanto phosphorus. Several lots of this material have been shown, by synthesis of InP, to be purer than others commercially available.

(2). To try different sources of HCl. A sample of Stauffer Chemical Company anhydrous HCl, reportedly[4] much purer than the Matheson HCl now in use, has been ordered. In addition, HCl will be generated by reduction of high purity PCl_3 or $AsCl_3$.

(3). To use a high purity alumina liner in the hot source and deposition zones. The alumina liner, boats and support plates are on hand.

(4). If further evaluation of GaP prepared by the H_2O transport process warrants it, to set up a furnace capable of operating continuously at the higher temperature and having a uniform cross sectional temperature profile. The latter feature is desirable in any case.

(5). Initiate trace analytical work on selected samples of GaP.

(6). Evaluate samples of GaP prepared by other methods.

(7). Continue examination of open circuit voltage-temperature relationship of GaP solar cells.

(8). Conclude optimizing phosphorus flow rate (P/Ga mole ratio) and crystal orientation with solar cell electrical and optical data.

(9). Measure temperature coefficient of energy gap $(\frac{dEg}{dT})$ of both indirect and direct gap of GaP by gold-GaP barrier photovoltage spectral measurements.

X. REFERENCES

1. F. V. Williams, J. Electrochem. Soc., to be published (July, 1964).
2. C. J. Frosch, J. Electrochem. Soc., 111, 180 (1964).
3. C. D. Thurmond and C. J. Frosch, J. Electrochem. Soc., 111, 184 (1964).
4. J. A. Amick, E. A. Roth and H. Gassenberger, R. C. A. Review, 24, 473 (1964); G. A. Lang and T. Stavish, ibid, 488.
5. T. S. Moss, "Optical Properties of Semiconductors" Butterworth's (1961) p. 224.
6. J. J. Wysocki and P. Rappaport, J. Appl. Phys., 31, 571 (1960).
7. A. R. Gobat, M. F. Lamorte, G. W. McIver, IRE Trans. Mil. Electronics, p. 20, January, 1962.

/gz

4-22-64

TABLE I

Epitaxial Deposition of GaAs[1]

Run and Sample No.	Source Temp (° C)	Substrate Temp (°C)	Substrate Grad. (°C/cm)	Flow Rates (cc/min) HCl	Flow Rates (cc/min) H_2	P/Ga Mole Ratio	Time (min)	Thickness μ	(μ/min)	(μ/ccHCl)	Orient
SC31-3	890	815	8	1.1	95	(5.4-1.9, $\overline{3.1}$)	300	30	.10	.13	<100>
-5		805	2.3					12	.04	.05	<100>
SC32-3	975	870	25	3.2	475	(1.5-0.44, $\overline{0.76}$)	332	130	.39	.12	<100>
-5		810	15					200	.60	.18	<100>
SC33-3	975[2]	835	24	2.2	300	(3.0-1.1, $\overline{1.7}$)	240	105	.44	.24	<100>
-5		790	13					97	.40	.22	<100>
SC34-3	895	825[3]	5.4	2.3	310	(2.3-0.83, $\overline{1.3}$)	303	35	.12	.062	<100>
-5		815[3]	3.0					30	.10	.053	<100>
SC35-3	890	810	9	2.3	310	(2.9-1.4, $\overline{2.0}$)	242	45	.19	.10	<100>
-5		800	2.9					30	.12	.067	<100>
SC36-3	905	830	7.0	2.2	300	3.12	282	55	.20	.12	<100>
-5		820	2.8					45	.16	.10	<100>
SC37-3	900	822	7.0	2.2	300	0.79	1229	250	.20	.11	<100>
-6		812	2.3					95	.077	.043	<111>B
-10		803	4.0					290	.24	.13	<111>A
SC38-4	900	812	3.4	2.2	300	0.49	1749	~ 170[4]	.10	.05	<111>A
-7		808	3.3					~ 12[4]	.007	.004	<100>
-10		787	5.6					~ 100[4]	.06	.03	<111>A
SC39-3	908	830	8.6	2.2	300	1.43	697	135	.19	.11	<100>
-6		816	3.3					180	.26	.14	<111>A
SC40-3	898	827	7.0	2.2	300	0.62	1616	115	.071	.037	<100>
-6		815	3.3					180	.11	.058	<111>A

(Continued next page)

TABLE I (Continued)

Epitaxial Deposition of GaAs[1]

Run and Sample No.	Source Temp (°C)	Substrate Temp (°C)	Substrate Grad. (°C/cm)	Flow Rates (cc/min) HCl	Flow Rates (cc/min) H_2	P/Ga Mole Ratio	Time (min)	Thickness μ	(μ/min)	(μ/ccHCl)	Orient
SC41-3	901	831	7.3	2.1	300	0.52	1655	100	.060	.03	<100>
-6		819[5]	3.4					25	.015	.008	<111>B
-8		812[5]	4.6					150	.090	.05	<111>A
-10		805[5]	5.3					140	.085	.045	<100>
SC42-3	904	817[6]	3.4	2.1	300	0.98	1070	165	.15	.08	<100>
-6		808	4.9					200	.19	.10	<111>B
-10		793	5.9					160	.15	.08	<111>B

(1) Source of elemental Ga and red P used in all runs.

(2) Sn, equivalent to 1.65×10^{19} atom/cc GaP added to Ga source.

(3) Substrate supported on massive graphite bar.

(4) Substrates extensively etched, extremely ragged interfaces and poor adhesion.

(5) Substrate wafers supported vertically, perpendicular to gas flow.

(6) Liquid Ga getter located in dump region just upstream from wafers.

TABLE II

Relative Growth Rates of GaP on Adjacent Substrates of Different Orientations

Hall Bar No.			Thickness (μ)			Ratio	
<100>	<111> B	<111> A	<100>	<111> B	<111> A	<111>B/<100>	<111>A/<100>
SC37-4 -5			181	105		0.58	
-8	-7	-9	106	90	358	0.85	3.38
SC39-4		-5	136		259		1.90
SC40-4		-5	73		184		2.52
SC41-4 -5			78.5	33.0		0.42	
SC42-4		-5	218		349		1.60
-8	-9	-7	156	128	349	0.82	2.24
-12	-11		215	194		0.90	

TABLE III

Properties of GaP Epitaxial Layers (N-type)

Sample No	Orient.	Thickness (μ)	ρ	μ	n
SC31-3	<100>	30	~ 10	(200)(1)	(2×10^{16})(1)
-5	<100>	12	~ 10	(800)(1)	(1×10^{17})(1)
SC32-3	<100>	130	0.54	94	1.9×10^{17}
-5	<100>	200	1.04	97	6.4×10^{16}
SC33-3	<100>	105	0.86	180	6.0×10^{16}
-5	<100>	97	1.40	100	4.6×10^{16}
SC34-3	<100>	35	5.9	76	1.4×10^{16}
-5	<100>	30	8.8	79	1.0×10^{16}
SC35-3	<100>	45	2.3	97	5.8×10^{16}
-5	<100>	30	13.0	69	1.9×10^{16}
SC36-3	<100>	55	2.3	97	2.8×10^{16}
-5	<100>	45	3.1	81	2.6×10^{16}
SC37-3	<100>	250	4.7	100	1.4×10^{16}
-6	<111> B	95	0.055	120	1.1×10^{18}
-10	<111> A	290	hi	-	-
SC38-4	<111> A	~ 170	102	53	1.2×10^{15}
-7	<100>	~ 12	(0.0070)(2)	(384)(2)	(2.34×10^{18})(2)
-10	<111> A	~ 100	114	29	1.9×10^{15}
SC39-3	<100>	135	3.9	96	2.1×10^{16}
-6	<111> A	180	2.8×10^{3}	10	2.5×10^{14}
SC40-3	<100>	115	10.2	98	1.5×10^{16}
-6	<111> A	180	hi	-	-
SC41-3	<100>	100	7.3	105	2.2×10^{16}
-6	<111> B	25	0.056	64	2.1×10^{18}
-8	<111> A	150	---------- Not Evaluated ----------		
-10	<100>	140	> 811(3)	< 46(3)	< 1.68×10^{14}(3)
SC-42-3	<100>	165	8.6	100	8.3×10^{15}
-6	<111> A	200	6×10^{3}	< 10	< 5×10^{14}
-10	<111> B	160	0.12	94	6.9×10^{17}

(1) Values unreliable due to extreme insensitivity in measurement.
(2) Probably spurious due to extensive etching of Hall bar substrate.
(3) Only first Hall bar measured, second was hi ρ

TABLE IV

Segregation of Impurities with Substrate Position
< 100 > Hall Bars

Run No.	Carrier Density (x 10^{-16})				Mobility			
	1st	2nd	3rd	4th	1st	2nd	3rd	4th
SC32	30.8	7.61	5.21		92	95	99	
SC33	8.71	3.28	6.11		235	133	75	
SC34	1.42	1.42	.688		67	85	73	
SC35	8.33	3.29	.426		123	71	67	
SC36	2.80	2.76	2.38		105	89	73	
SC37	1.67	1.14			105	94		
SC39	3.11	1.16			99	94		
SC40	2.57	0.484			126	70		
SC41	4.0	0.474	0.168	(hi ρ)	111	100	46	(hi ρ)
SC42	1.06	0.596	0.279	0.208	115	87	60	33

TABLE V

Electrical Properties of GaP Grown on Adjacent Substrates of Different Orientations

Hall Bar No.			Carrier Density			Mobility			Carrier Ratio
<100>	<111>B	<111>A	<100>	<111>B	<111>A	<100>	<111>B	<111>A	<111>B/<100>
SC37-4 -5			1.14×10^{16}	1.68×10^{18}		94	84		147
-8	-7	-9	(±)	5.90×10^{17}	(hi ρ)	(±)	162	(hi ρ)	-
SC39-4		-5	1.16×10^{16}		1.4×10^{14}	99		13	
SC40-4		-5	4.8×10^{15}		(hi ρ)	70		(hi ρ)	
SC41-4	-5		4.74×10^{15}	1.31×10^{18}		100	61		276
	-7			2.80×10^{18}			67		
SC42-4		-5	5.96×10^{15}		(hi ρ)	87		(hi ρ)	
-8	-9	-7	2.79×10^{15}	1.50×10^{18}	5.1×10^{14}	60	66	10	538
-12	-11		2.08×10^{15}	2.79×10^{17}		33	123		134

TABLE VI

Solar Cell Fabrication Diffusion Data

Diff. Run No.	Slice No.	Diffusant Source and Amt.	Diff Temp (°C)	Diff Time (Min)	P Surface Conc/cm^3	μ of P Layer cm^2/volt sec.	Junction Depth μ
NA26	SC27-3	5.8 mg Zn, 1.8 mg P	800	3	3.3×10^{18}	27	1.5
NA26	SC28-3	"	800	3	4.9×10^{18}	27	1.0
NA26	SC29-3	"	800	3	----- No jct. found ----------		
NA26	SC30-3	"	800	3	6.5×10^{18}	24	0.7
NA27	SC19-3	5 mg (95% Ga, 5% Zn)	800	3	-	-	0.5
NA27	SC25-3	"	800	3	4.5×10^{17}	100	0.5
NA28	SC13-6	"	800	3	9.6×10^{17}	4	0.5
NA28	SC17-3	"	800	3	8×10^{17} (N)	18	1.0
NA28	SC19-3	"	800	3	8.6×10^{18}	.1 (?)	0.5
NA28	SC19-5	"	800	3	Surface resistivity too high		0.5 (?)
NA28	SC26-3	"	800	3	5.8×10^{18}	91	0.5
NA29	SC31-5	5.8 mg Zn, 1.8 mg P	800	3	1.2×10^{19}	24	0.5
NA30	SC31-3	"	800	3	7×10^{18}	18	0.5
NA30	SC32-3	"	800	3	7.8×10^{18}	13	0.5
NA30	SC32-5	"	800	3	7.5×10^{18}	17	0.5
NA31	SC33-3	"	800	3	4.2×10^{18}	22	1.0
NA31	SC33-5	"	800	3	5.6×10^{18}	22	0.8
NA31	SC34-3	"	800	3	2.5×10^{18}	23	1.5
NA32	SC34-5	"	800	3	7.2×10^{18}	15	2.0
NA32	SC35-3	"	800	3	2.3×10^{19}	18	0.5
NA32	SC35-5	"	800	3	8.4×10^{18}	12	1.0

(Continued next page)

TABLE VI (Continued)

Solar Cell Fabrication Diffusion Data

Diff. Run No.	Slice No.	Diffusant Source and Amt.	Diff Temp (°C)	Diff Time (Min)	P Surface Conc/cm^3	μ of P Layer cm^2/volt sec.	Junction Depth μ
NA33	SC36-3	5.8 mg Zn, 1.8 mg P	800	3	6.8×10^{18}	13	0.5
NA33	SC36-5	"	800	3	1.4×10^{18}	40	1.5
NA33	SC37-3	"	800	3	2.5×10^{18}	18	1.0
NA33	SC37-6	"	800	3	2.0×10^{19}	2 (?)	0.5
NA34	SC38-4	"	800	3	3.2×10^{18}	23	0.5
NA34	SC38-7	"	800	3	No measurable values obtained		
NA34	SC38-10	"	800	3	1.5×10^{18}	21	1.0
NA34	SC39-3	"	800	3	1.8×10^{18}	21	1.0
NA34	SC39-6	"	800	3	9.2×10^{17}	21	0.5
NA34	SC40-3	"	800	3	1.5×10^{18}	21	1.5
NA34	SC40-6	"	800	3	3.5×10^{18}	26	0.5

TABLE VII

Comparison of Solar Cell Parameters using the Sun and Tungsten Light Sources

Temperature = 25° C.

Sample	J_{sc} (ma/cm²)		V_{oc} (Volts)		Conversion Efficiency (using Sun)	Area of Samples (cm²)
	Sun	Tungsten	Sun	Tungsten		
NA16SC14-2	.30	.04	1.05	1.0	-	.22
NA21SC18-5	.69	.08	1.1	1.08	-	.20
NA21SC19-3	.89	.14	1.0	1.0	.75%	.25
NA21SC19-5	.73	.09	1.05	.96	-	.13
NA25SC22-3	.25	.06	.83	.90	-	.36
NA21-SC21-3	5	5	.70	.74	-	.09
NA25SC23-3	.21	.06	1.05	1.05	-	.20
NA25SC25-3	1.2	.19	1.08	.92	1%	.24
NA21SC20-3	.26	.06	1.0	.92	-	.25
NA26SC27-3	.81	.14	1.1	1.04	-	.25
NA25SC26-3	.11	.13	.92	.90	-	.39

TABLE VIII

Relationship of Growing Conditions, Short Circuit Current, Spectral Response Peaks for GaP Solar Cells

Run No.	Slice No.	H_2 Flow Rate cc/min	Source Temp °C.	Spectral Response Peaks (Microns)				J_{sc} (ma/cm²) ± Sunlight
NA21	SC21-3	15	890				0.77	5.0
NA30	SC31-3	95	890	0.45				1.2
NA29	SC31-5	95	890		0.50		0.7	0.10
NA16	SC14-2	150	890	0.46	0.50			0.30
NA20	SC15-3	150	890		0.53			0.025
NA20	SC17-3	150	890		0.53		0.76	0.28
NA21	SC19-3	150	890	0.45	0.50			0.89
NA21	SC19-5	150	890	0.45				0.73
NA25	SC25-3	150	890	0.45				1.2
NA26	SC27-3	170	890	0.45				0.81
NA26	SC28-3	170	890	0.45				1.15
NA21	SC20-3	300	890	0.45				0.26
NA31	SC34-3	310	895	0.45				1.43
NA32	SC34-5	310	895	0.45				0.76
NA25	SC22-3	500	890	0.45				0.25
NA25	SC23-3	500	890	0.45				0.21
NA25	SC24-5	500	890	0.45				0.29
NA16	SC13-6	150	935	0.45	0.53	0.59	0.7	0.03
NA20	SC13-4	150	935	0.46	0.54		0.7	0.16
NA25	SC26-3	150	975	0.46	0.54			0.11
NA26	SC29-3	150	975		0.53			0.06
NA30	SC32-3	475	975	0.44			0.7	0.66
NA30	SC32-5	475	975	0.45	0.53	0.58*	0.8	1.0
NA26	SC30-3	800	975	0.45	0.55*		0.8	0.67

± Measurements made from open window between 11:00 a.m. and 3:00 p.m. with sample pointed toward sun. A 10% standard silicon solar cell was also measured at the same time to provide an idea of the solar intensity level - if the incident intensity was lower than 80 mw/cm² measurements were not taken.

* Negative response

TABLE IX

Relationship between Epitaxial Growth Conditions and Temperature Dependence of Short Circuit Current for Cells having only 0.45 μ Response

Run No.	Slice No.	H_2 Flow Rate cc/min	Source Temp. ° C	J_{sc} (ma/cm^2) (Sunlight)	Slope, ΔE (ev) J_{sc} vs. 1/T	Conversion* Efficiency
NA30	SC31-3	95	890	1.2	Indeterminate	0.45 %
NA21	SC19-5	150	890	0.73	.045	-
NA25	SC25-3	150	890	1.2	.044	1.0%
NA26	SC27-3	170	890	0.81	.05	-
NA26	SC28-3	170	890	1.15	.047	1.1%
NA21	SC20-3	300	890	0.26	.07	-
NA31	SC34-3	310	895	1.43	.06	1.1%
NA32	SC34-5	310	895	0.76	.06	0.7%
NA25	SC22-3	500	890	0.25	.04, .08	-
NA25	SC23-3	500	890	0.21	.08	-
NA25	SC24-5	500	890	0.29	.04, .08	-

* See footnote of Table VIII concerning solar measurement.

TABLE X

Relationship between Phosphorus Flow Rate used in Epitaxial Growth and Solar Cell Properties

Run No.	Slice No.	Phosphorus $\pm$ Flow Rate (cc/min)	P/Ga Mole Ratio	V_{oc} ** (Volts)	J_{sc} ** ma/cm^2	Spectral Response Peaks Microns
NA33	SC36-3	1.28	3.12	0.52	0.74	0.45, 0.6*, 0.7
NA33	SC36-5	1.28	3.12	0.64	0.50	0.45, 0.7*
NA33	SC37-3	0.36	0.79	1.20	0.78	0.45
NA34	SC39-3	0.647	1.43	1.35	1.13	0.45
NA34	SC40-3	0.30	0.62	1.30	1.05	0.45
NA35	SC41-3	0.24	0.52	1.30	-	0.45

$\pm$ Source temp., H_2, HCl flow rates maintained constant, fixed orientation < 100 > .

* Negative Response.

** Measured in sunlight.

TABLE XI

Relationship between V_{knee}, Spectral Response and V_{oc}

Run No.	Slice No.	V_{knee} (Volts) (from I_f - V_f Trace)	Spectral Response Peaks (Microns)	V_{oc} (Volts) (Sunlight)	J_{sc} (ma/cm^2) (Sunlight)
NA26	SC27-3	1.1	0.45,	1.17	0.81
NA26	SC28-3	1.2	0.45,	1.27	1.15
NA25	SC25-3	1.1	0.46,	1.05	1.2
NA30	SC31-3	1.3	0.45,	1.30	1.2
NA16	SC13-6	0.9	0.46, 0.53, 0.59, 0.7	0.58	0.03
NA23	SC13-6	1.6	0.53, 0.6 0.7	0.50	0.03
NA20	SC13-4	1.1	0.46, 0.54, 0.7	0.76	0.16
NA20	SC15-3	3	0.53,	0.80	0.03
NA27	SC25-3	1.6	0.45, 0.53, 0.75	1.0	0.30
NA26	SC30-3	6	0.45, 0.55*, 0.8	0.62	0.67
NA28	SC26-3	12	0.58, 0.75	0.79	0.05
NA25	SC26-3	5	0.46, 0.53	0.95	0.29
NA29	SC31-5	0.8	0.50 0.70	0.92	0.10
NA30	SC32-5	4.5	0.45, 0.53, 0.58* 0.8	0.92	1.0
NA30	SC32-3	0.7	0.44 0.7	0.90	0.66

* Negative Response.

TABLE XII

Solar Cell Evaluation Data at Room Temperature

Diff. Run No.	Slice No.	Spectral Response Peaks Microns λ_1	λ_2	λ_3	J_{sc} (ma/cm²) Sun	J_{sc} (ma/cm²) Tungsten	V_{oc} (Volts) Sun	V_{oc} (Volts) Tungsten	Area of Samples Cm²	Conversion Efficiency ** (using sun)
NA26	SC27-3	0.45			.81	.14	1.10	1.04	.25	-
NA26	SC28-3	0.45			1.2	.13	1.30	1.10	.10	1.1%
NA26	SC29-3		0.53		.06	.02	.68	.64	.16	-
NA26	SC30-3	0.45	0.55*	0.7 (broad)	.67	.08	.62	.31	.20	-
NA27	SC19-3	0.45	0.53		.13	.03	.82	.74	.11	-
NA27	SC25-3		0.53	0.8	.30	.07	1.0	.92	.10	-
NA28	SC13-6	0.43	0.52	0.8	.28	.11	.92	.82	.19	-
NA28	SC17-3	0.43	0.50		.007	.007	.05	.04	.14	-
NA28	SC19-3	----------Sample Broke ----------								
NA28	SC19-5	0.44	0.50		.14	.27	.91	.92	-	-
NA28	SC26-3		0.6	0.75 (broad)	.03	.04	.79	.78	.31	-
NA29	SC31-5		0.50	0.7	.10	.03	.92	.91	.26	-
NA30	SC31-3	0.45			1.2	.17	1.29	1.15	.03	0.45%
NA30	SC32-3	0.44		0.7 (broad)	.66	.07	.90	.90	.09	-
NA30	SC32-5	0.45	0.55*	0.7	1.0	.14	.92	.54	.17	-
NA31	SC33-3	0.45			0.61	.11	1.10	.94	.39	-
NA31	SC33-5	0.45			0.92	.13	1.30	1.00	.54	0.75%
NA31	SC34-3	0.45			1.43	.23	1.35	1.10	.57	1.1%
NA32	SC34-5	0.45			1.30	.15	0.76	1.20	.27	0.7%
NA32	SC35-3	0.45	0.50	0.8	0.54	.08	1.24	1.00	.48	-

Continued next page

TABLE XII (Continued)

Solar Cell Evaluation Data at Room Temperature

Diff Run No.	Slice No.	Spectral Response Peaks Microns λ_1	λ_2	λ_3	J_{sc} (ma/cm²) Sun	Tungsten	V_{oc} (Volts) Sun	Tungsten	Area of Samples Cm²	Conversion Efficiency ** (using sun)
NA32	SC35-5	0.45	0.50		0.88	.13	1.26	1.20	.43	0.6%
NA33	SC36-3	0.45	0.60*	0.7	0.74	.15	.52	.38	.23	-
NA33	SC36-5	0.45		0.7*	.50	.14	.64	.58	.30	-
NA33	SC37-3	0.45			.78	.12	1.20	1.12	.10	-
NA33	SC37-6	0.45			.20	.03	.96	.94	.20	-
NA33	SC37-10	----------No Output----------								
NA34	SC38-4	0.53			.04	.01	.83	.83	.18	-
NA34	SC38-7	----------No Output----------								
NA34	SC38-10	----------No Output----------								
NA34	SC39-3	0.45			1.13	.15	1.35	1.02	.22	-
NA34	SC39-6		0.53		.00	.00	1.10	.99	.26	-
NA34	SC40-3	0.45			1.05	.14	1.30	1.10	.20	-
NA34	SC40-6		0.53		.06	.00	1.20	1.12	.17	-

* Negative response.

** See footnote of Table VIII concerning solar measurement.

TABLE XIII

Data on Solar Cells Delivered to Lewis Research Center

Sample.	NA31 SC34-3	NA31 SC33-5	NA32 SC34-5	NA22 SC21-3
Growth Conditions:				
Source Temp. (°C)	895	975	895	890
Substrate Temp. (°C)	825	790	815	815
H_2 Flow Rate (cc/min)	310	300	310	15
HCl Flow Rate (cc/min)	2.3	2.2	2.3	0.92
P_4 Flow Rate (cc/min)	.9	.78	.9	2.0
Layer thickness (μ)	35	97	30	10
η Carrier Conc. (No./cm^3)	1.4×10^{16}	4.6×10^{16}	1.1×10^{16}	P-type **
μ (cm^2/volt sec)	76	100	79	-
ρ (ohm-cm)	5.9	1.40	8.8	-
Diffusion:				
Dopant	zinc	zinc	zinc	zinc
Temp (°C)	800	800	800	800
Time (min)	3	3	3	10
Cell Evaluation:				
P-layer conc. (No./cm^3)	2.5×10^{18}	5.6×10^{18}	7.2×10^{18}	1.1×10^{19}
μ (cm^2/volt sec)	23	22	15	31
Jct. Depth (μ)	1.5	~0.8	2.0	4
Forward I-V Trace, V_{knee} (Volts)	1.1	1.2	1.2	.6
Max. Power (in sun) (mw)	.608 *	.38 *	.182 *	.224 ±
V_{oc} (Volts)	1.35	1.30	1.30	0.58
J_{sc} (ma/cm^2)	1.43	0.92	0.76	4.0
Cell area (cm^2)	0.57	0.54	0.27	0.18
Efficiency (in sun) (relative to std. Si solar cell), (%)	1.1*	0.75*	0.7*	1.68 ±
Spectral Response (μ)	0.45	0.45	0.45	0.75 (broad)
Slope J_{sc} vs. $1/T$ (ev)	.06	.06	.06	-
D.C. I_f-V_f: $I_o \exp \frac{ev}{nkT}$; n	4	6	5	2

* Based on solar intensity, as measured with Si solar cell, of 94 mw/cm^2.

** From C-V data.

± Based on solar intensity, as measured with Si solar cell, of 74 mw/cm^2.

TABLE XIV

Open Circuit Voltage* vs. Temperature

Sample	V_{oc} (23° C)	Temp. Coefficient (β) mv/°C	t_m (°C) Max. Temp.	V_{oc} at t_m (°C)	n_i Initial
NA31 SC34-3	1.15	3.5	225	0.5	1.4×10^{16}
NA32 SC34-5	1.2	2.78	225	0.63	1.05×10^{16}
NA31 SC33-5	1.0	2.5	225	0.6	4.6×10^{16}
NA26 SC28-3	1.15	3.0	350	0.28	2.7×10^{16}
NA26 SC27-3	1.05	2.83	350	0.26	4.8×10^{16}
NA30 SC31-3	1.20	4.4	325	0.07	2×10^{16}
NA21 SC20-3	.96	3.74	275	0.12	1.5×10^{18}
NA33 SC37-3	1.20	2.88	350	0.36	1.4×10^{16}
NA33 SC37-6	.96	2.75	350	0.20	1.1×10^{18}
NA34 SC40-3	1.24	2.8	350	0.40	1.5×10^{16}

* Measured with tungsten source or sunlight.

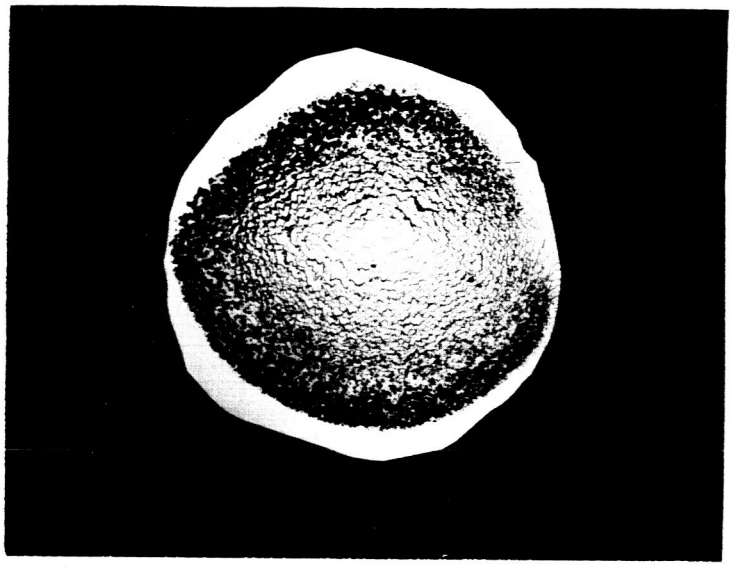

Figure 1: SC37-10 Typical Growth on < 111 > A Surface. Edge 370 μ, Center 215 μ

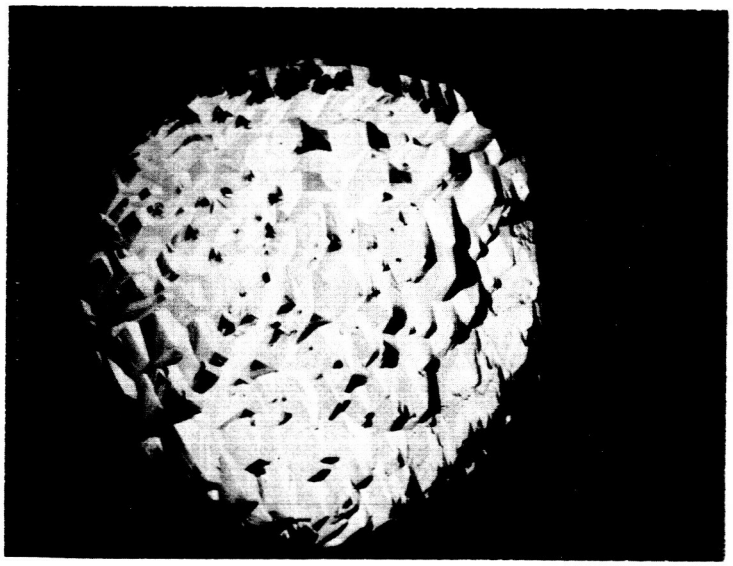

Figure 2: SC37-6 Typical Growth on < 111 > B Surface. ~ 95 μ

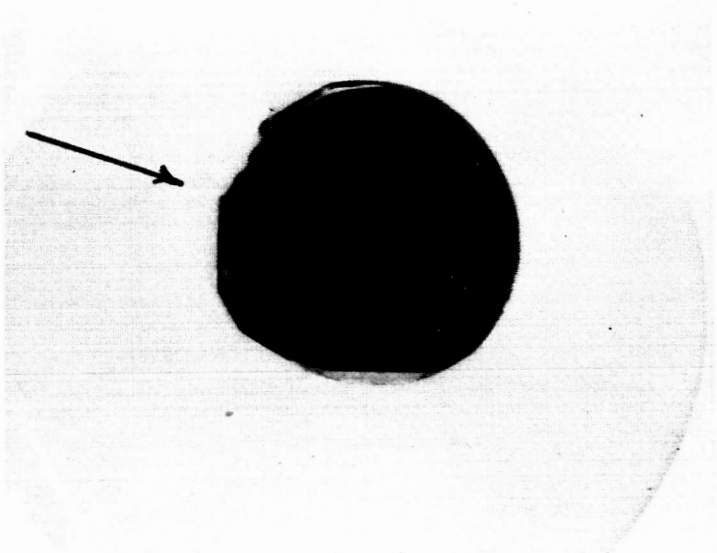

Figure 3: SC44-2 Growth on < 111 > B Surface by H_2O transport. Note < 110 > facets.

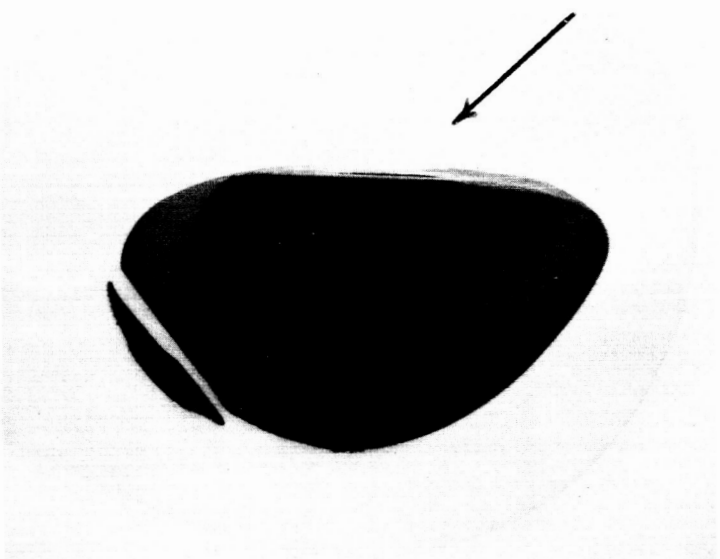

Figure 4: SC44-5 Growth on < 100 > Surface by H_2O transport. Sides heavily etched. Arrow shows direction of gas flow.

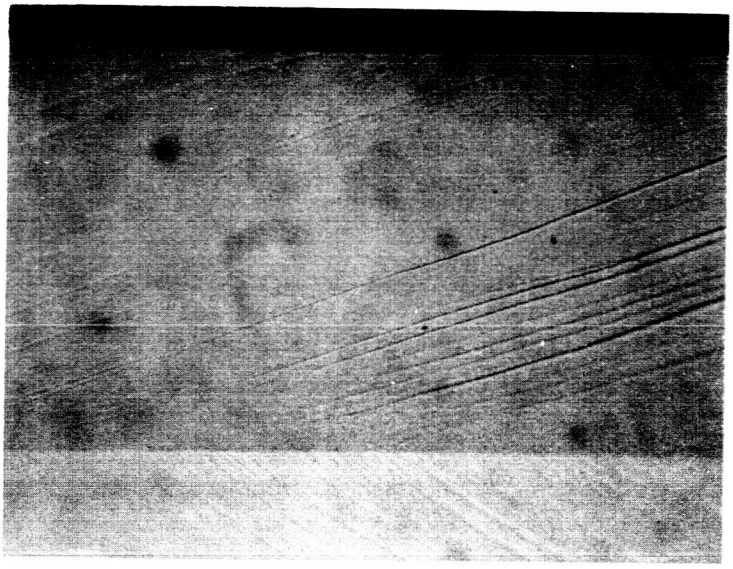

Figure 5: SC44-3 Spontaneously cleaved section of GaP layer grown by H_2O transport on GaAs. Not etched. 500X.

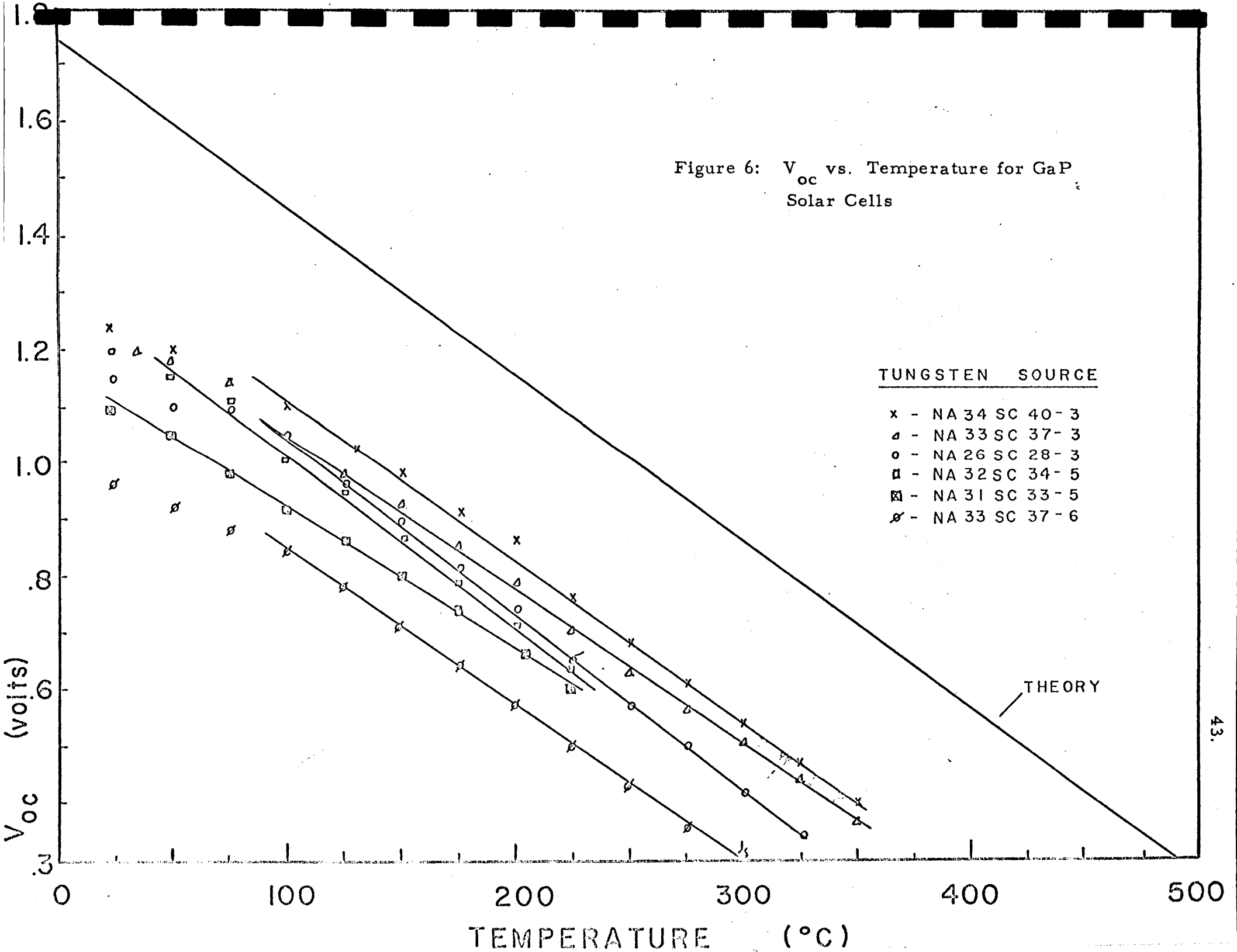

Figure 6: V_{oc} vs. Temperature for GaP Solar Cells

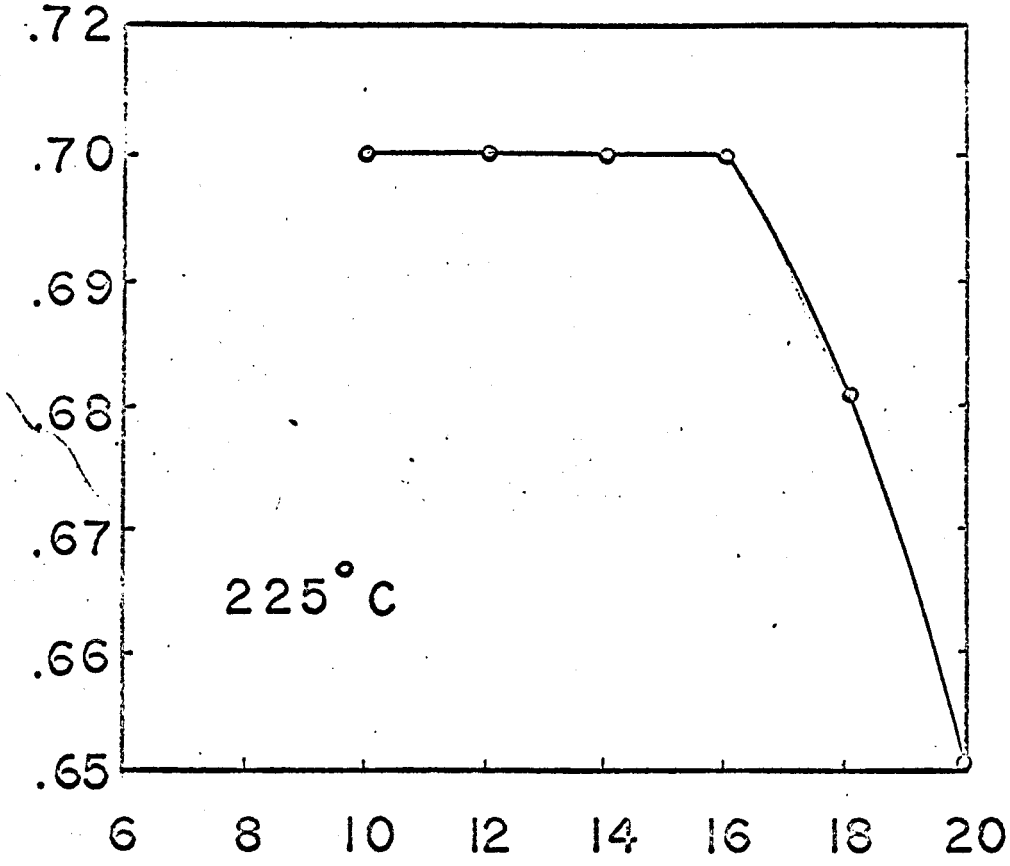

Figure 7: V_{oc} vs. Source-Sample Separation with Tungsten Source At Room Temperature and 225° C.

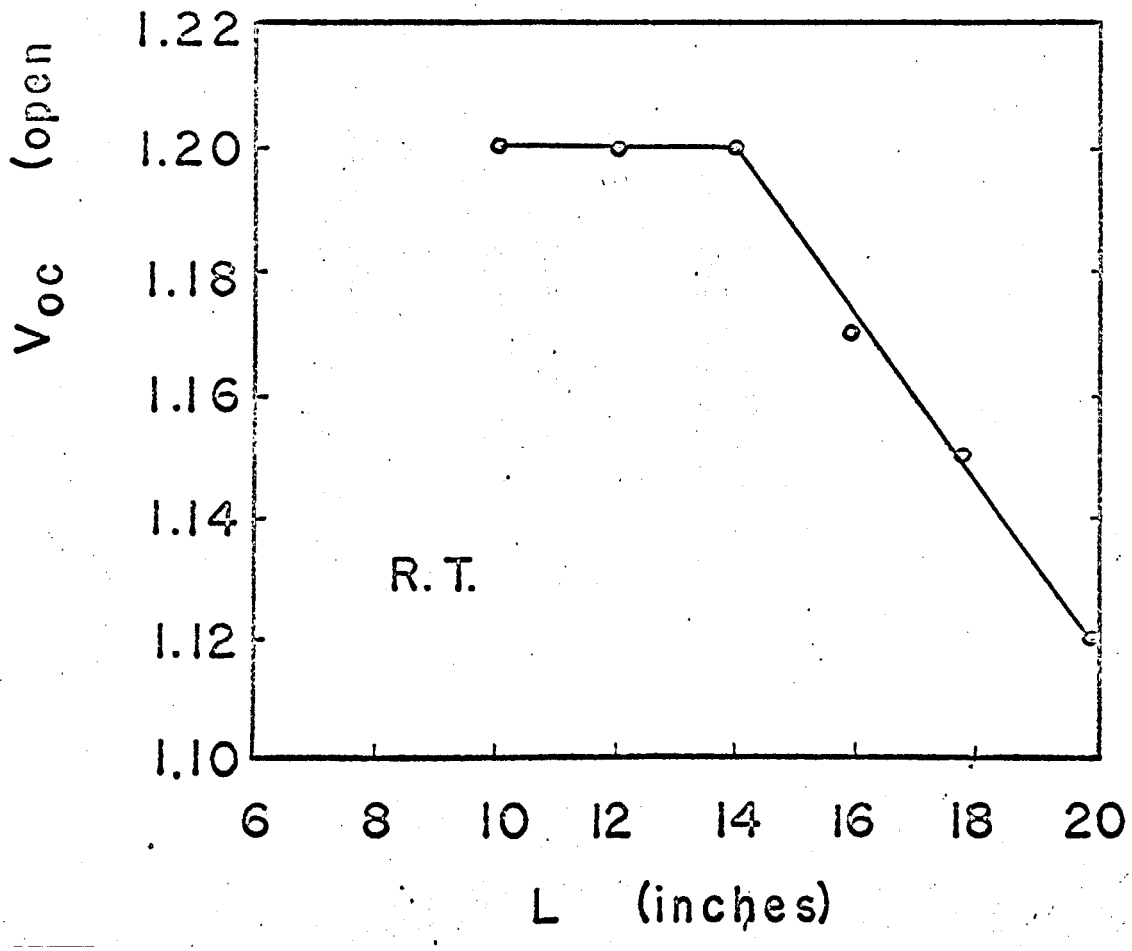

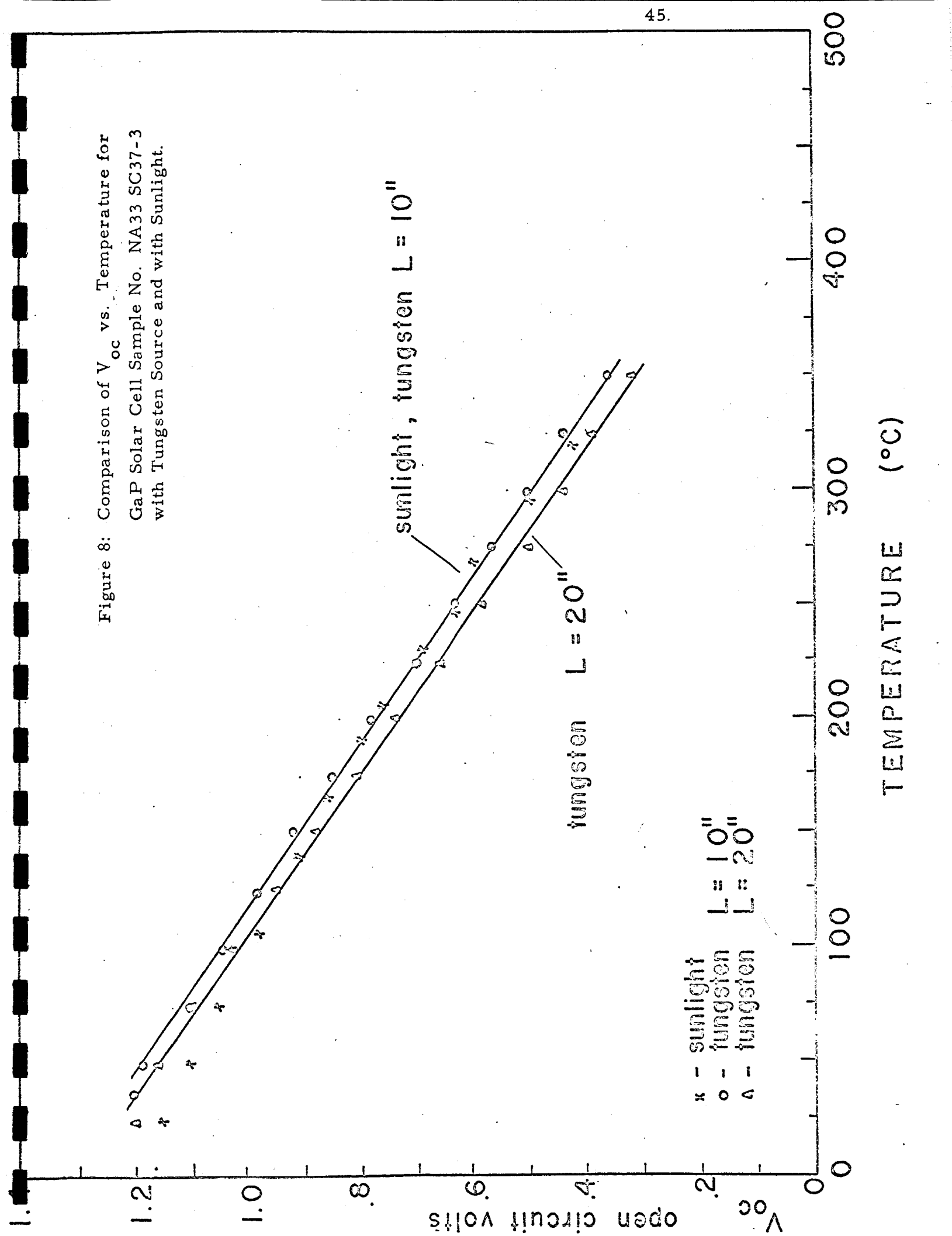

Figure 8: Comparison of V_{oc} vs. Temperature for GaP Solar Cell Sample No. NA33 SC37-3 with Tungsten Source and with Sunlight.

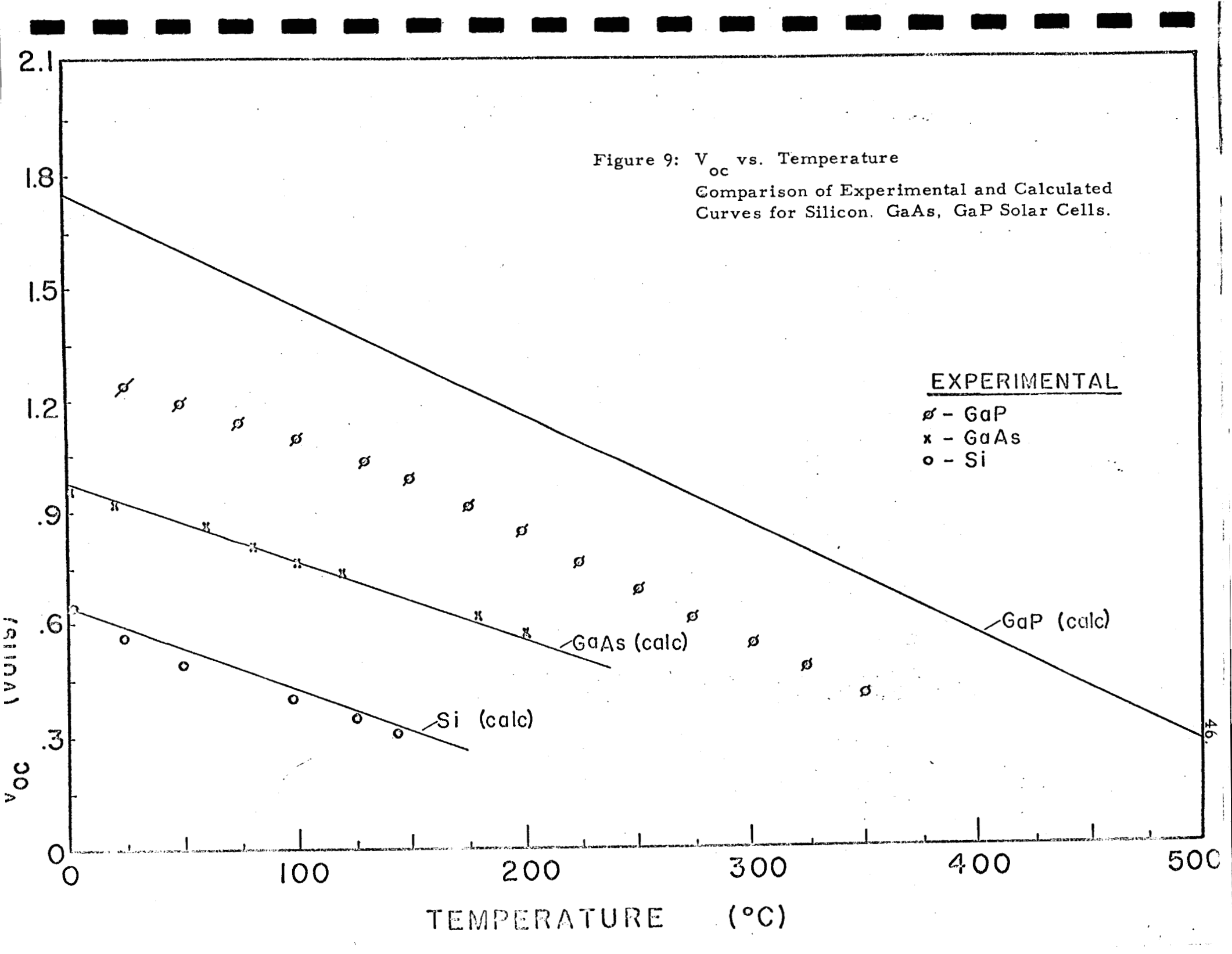

Figure 9: V_{oc} vs. Temperature
Comparison of Experimental and Calculated Curves for Silicon, GaAs, GaP Solar Cells.

DISTRIBUTION LIST

		Number of Copies
National Aeronautics and Space Administration Washington, D. C. 20546		
Attn:	Walter C. Scott/RP	1
	J. L. Sloop/RP	1
	Millie Ruda/AFSS-LD	1
National Aeronautics and Space Administration Scientific and Technical Information Facility Box 5700 Bethesda, Maryland 20546		3
National Aeronautics and Space Administration Goddard Space Flight Center Greenbelt, Maryland 20771		
Attn:	W. R. Cherry	1
	M. Schach	1
	B. Mermelstein, Code 672	1
	J. W. Callaghan, Code 621	1
	Librarian	1
National Aeronautics and Space Administration Lewis Research Center 21000 Brookpark Road Cleveland, Ohio 44135		
Attn:	J. J. Fackler, MS 86-1	1
	B. Lubarsky, MS 86-1	1
	H. Shumaker, MS 86-1	1
	R. L. Cummings, MS 86-1	1
	C. [illegible]. Swartz, MS 86-1	4
	N. D. Sanders, MS 302-1	1
	J. Broder, MS 302-1	1
	J. Mandelkorn, MS 302-1	1
	A. E. Potter, MS 302-1	1
	C. S. Corcoran, MS 100-1	1
	N. T. Musial, MS 77-1	1
	George Mandel, MS 5-5	1
National Aeronautics and Space Administration Langley Research Center Langley Station Hampton, Virginia 23365		
Attn:	W. C. Hulton	1
	E. Rind	1

DISTRIBUTION LIST

		Number of Copies
Jet Propulsion Laboratory 4800 Oak Grove Drive Pasadena, California 91103		
Attn:	P. Goldsmith	1
	G. E. Sweetnam	1
Institute for Defense Analysis Connecticut Avenue, N. W. Washington, D. C. 20546		
Attn:	R. Hamilton	1
Advanced Research Projects Agency Department of Defense, Pentagon Washington, D. C. 20546		
Attn:	Dr. C. Yost	1
Naval Research Laboratory Department of the Navy Washington, D. C. 20546		
Attn:	E. Broncato, Code 6464	1
	M. Wotaw, Code 5170	1
	Dr. L. Linnenbom, Code 7450	1
	Dr. C. Klick, Code 6440	1
U. S. Army Advent Management Agency Mission Equipment Department Ft. Monmouth, New Jersey		
Attn:	William Scherr, SIGFM/PAM-5	1
U. S. Army Signal Research and Development Laboratory Fort Monmouth, New Jersey		
Attn:	Power Sources Branch	1
Air Force Cambridge Research Center Air Research and Development Command USAF, Hanscem Field Bedford, Massachusetts		
Attn:	Col. G. de Giacomo	1
Air Force Ballistic Missile Division Air Force Unit Post Office Los Angeles 45, California		
Attn:	COL. L. Norman, SSEM	1
	LT. COL. G. Austin, SSZAS	1
	CAPT. A. Johnson, SSZDT	1
	CAPT. W. Hoover, SSTRE	1
	LT. COL. A. Bush, SSZME	1

DISTRIBUTION LIST

		Number of Copies
Wright Air Development Division Wright-Patterson Air Force Base Dayton, Ohio		
Attn:	P. R. Betheand	1
	Mrs. E. Tarrants/WWRNEM-1	1
Flight Accessories Aeronautics Systems Division Wright-Patterson AFB Dayton, Ohio		
Attn:	Joe Wise/ASRMFP-2	1
Aerospace Corporation P. O. Box 95085 Los Angeles 45, California		
Attn:	Dr. G. Hove	1
	Dr. F. Mozer	1
	V. J. Porfune	1
	Dr. I. Spiro	1
Battelle Memorial Institute 505 King Avenue Columbus, Ohio		
Attn:	L. W. Aukerman	1
	R. E. Bowman	1
	T. Shielladay	1
Bell and Howell Research Center 360 Sierre Madre Villa Pasadena, California		
Attn:	Alan G. Richards	1
Bell Telephone Laboratories Murray Hill, New Jersey		
Attn:	W. L. Brown	1
	U. B. Thomas	1
Clevite Research Center 540 E. 105th Street Cleveland Ohio 44108		
Attn:	Dr. Hans Jaffe	1
The Eagle-Picher Company Chemical and Material Division Miami Research Laboratories 200 Ninth Avenue, N. E. Miami, Oklahoma		
Attn:	John R. Musgrave	1

DISTRIBUTION LIST

	Number of Copies
Harshaw Chemical Company Solid-State Division 2240 Prospect Avenue Cleveland, Ohio 44115 Attn: James C. Schaefer	1
Heliotek Corporation 12500 Gladstone Avenue Sylmar, California Attn: Eugene Ralph	1
Hughes Aircraft Company Aerospace Group, R and D Division Culver City, California Attn: C.A. Escoffery	1
Leesona Moos Laboratories 90-28 Van Wyck Expressway Jamaica 18, New York Attn: Stanley Wallack	1
National Cash Register Company Physical Research Department Dayton 9, Ohio Attn: R. R. Chamberlin	1
North American Aviation, Inc. Autonetics Division Anaheim, California Attn: R. R. August	1
Philco Corporation Blue Bell, Pennsylvania Attn: Mr. A. E. Mace	1
Radio Corporation of America RCA Research Laboratories Princeton, New Jersey Attn: P. Rappaport	1
Radio Corporation of America Semiconductor and Materials Division Somerville, New Jersey Attn: Dr. F. L. Vogel	1

DISTRIBUTION LIST

	Number of Copies
Sandia Corporation Albuquerque, New Mexico Attn: F. Smits	1
Solid-State Electronics Laboratory Stanford Electronics Laboratory Stanford University Stanford, California Attn: Prof. G. L. Pearson	1
Westinghouse Electric Corporation Research and Development Laboratories Churchill Borough, Pennsylvania Attn: H. C. Chang	1
Westinghouse Electric Corporation Semiconductor Division Youngwood, Pennsylvania Attn: Don Gunther	1
Massachusetts Institute of Technology Security Records Office Room 14-0641 Cambridge 39, Massachusetts	1